Diatom Research
Publication details, including instructions for authors and subscription information:
http://www.tandfonline.com/loi/tdia20

Photoprotective function of mycosporine-like amino acids in a bipolar diatom (Porosira glacialis): evidence from ultraviolet radiation and stable isotope probing

Sun-Yong Ha[a], Hyoung Sul La[a], Jun-Oh Min[a], Kyung-Ho Chung[a], Sung-Ho Kang[a] & Kyung-Hoon Shin[b]

[a] Division of Polar Marine Environment, Korea Polar Research Institute (KOPRI), Incheon, South Korea

[b] Marine Environmental Science Department, Hanyang University, Kyeonggi-do, Korea

Published online: 18 Mar 2014.

To cite this article: Sun-Yong Ha, Hyoung Sul La, Jun-Oh Min, Kyung-Ho Chung, Sung-Ho Kang & Kyung-Hoon Shin (2014): Photoprotective function of mycosporine-like amino acids in a bipolar diatom (Porosira glacialis): evidence from ultraviolet radiation and stable isotope probing, Diatom Research, DOI: 10.1080/0269249X.2014.894945

To link to this article: http://dx.doi.org/10.1080/0269249X.2014.894945

Diatom Research, 2014
http://dx.doi.org/10.1080/0269249X.2014.894945

Taylor & Francis
Taylor & Francis Group

Photoprotective function of mycosporine-like amino acids in a bipolar diatom (*Porosira glacialis*): evidence from ultraviolet radiation and stable isotope probing

SUN-YONG HA[1]*, HYOUNG SUL LA[1], JUN-OH MIN[1], KYUNG-HO CHUNG[1], SUNG-HO KANG[1] & KYUNG-HOON SHIN[2]

[1]*Division of Polar Marine Environment, Korea Polar Research Institute (KOPRI), Incheon, South Korea*
[2]*Marine Environmental Science Department, Hanyang University, Kyeonggi-do, Korea*

This study investigated the synthesis of photoprotective compounds by Bacillariophyceae (*Porosira glacialis*) in real time using a ^{13}C tracer. Our results show a relationship between the net production rates of mycosporine-like amino acids (MAAs) and photoprotective pigments such as diadinoxanthin (DD). After 24 h, the total carbon uptake rate of *P. glacialis* was higher when exposed to photosynthetically active radiation (PAR) than when exposed to ultraviolet radiation (UVR). However, with time, the total carbon uptake rate and turnover rate of *P. glacialis* exposed to UVR increased to the point where the net production rate of MAAs under UVR was higher than that of *P. glacialis* exposed to PAR. The differences in MAA and DD production rates and carbon uptake indicate the production of MAA and DD as a defense strategy in response to UV-induced damage. The results of this study provide insight into the synthetic pathways of photoprotective compounds and the carbon cycle within *P. glacialis* cells and reveal contrasting patterns in the production of MAAs and xanthophyll compounds such as DD over time.

Keywords: *carbon stable isotope, mycosporine-like amino acids, xanthophyll compound,* Porosira *glacialis*

Introduction

Ultraviolet radiation (UVR) inhibits photosynthesis and the primary productivity of phytoplankton (*Helbling* et al. 1992, Häder et al. 2007) and adversely affects protein synthesis and DNA in cells (Karentz et al. 1991). Moreover, UVR interferes with the absorption of nutrients (Behrenfeld et al. 1995) and affects the biochemistry of various types of cellular enzymes (Sinha & Häder 2002). The effects of UVR on the metabolism or survival of phytoplankton cells vary significantly by species according to their abilities to adapt to UV exposure and repair damaged DNA (Karentz et al. 1991).

The production of photoprotective compounds is a means by which aquatic organisms can protect themselves against strong light and UVR, and has been shown to enable survival in extreme environments (Moeller et al. 2005). Since they absorb radiation between 310 and 362 nm, mycosporine-like amino acids (MAAs) can function as photoprotectants in phytoplankton that are exposed to harmful natural light (Häder et al. 2007), and have been shown to protect intracellular organs against UVR (Karentz 2001, Whitehead et al. 2001, Volkmann & Gorbushina 2006). Xanthophyll pigments, which are located in the cytoplasm, act as a passive sunscreen (Garcia-Pichel & Castenholz 1993).

Several studies have reported a relationship between xanthophyll pigments and MAAs with respect to UVR (Shinha et al. 2003, Ha et al. 2010, Korbee et al. 2010). Ha et al. (2010) suggested that the concentration of DD, a xanthophyll compound found in *P. glacialis*, decreases as the concentration of MAAs increases with the length of exposure to artificial UV. As protectants, the two types of compounds are complementary. MAAs act by absorbing UV light, and xanthophylls act by scattering light energy (Demming-Adams & Adams 1996, Sinha et al. 2003). However, this relationship between photoprotective compounds may depend on the phytoplankton species involved or on environmental factors (Ha et al. 2010, Korbee et al. 2010). Korbee et al. (2010) reported that, in *Heterocapsa* spp. (Dinophyta), excess energy caused by UVR exposure is converted to heat when nitrogen is not a limiting factor, resulting in the accumulation of MAAs (Conde et al. 2004). However, when nitrogen is limiting, MAA content decreases and excess energy is instead de-epoxidized by xanthophyll cycle pigments. Zudaire & Roy (2001) reported that the coastal diatom *Thalassiosira weissflogii* is a relatively UV-tolerant species; the xanthophyll cycle is activated, and MAAs are synthesized when photoinhibition is relieved.

*Corresponding author. E-mail: sundragon@kopri.re.kr

(Received 8 October 2013; accepted 7 January 2014)

Goericke & Welschmeyer (1993) reported a method for measuring specific rates of chlorophyll synthesis using a ^{14}C tracer. The method determines the amount of assimilated inorganic carbon by measuring the amount of newly fixed carbon incorporated into all cellular constituents. When inorganic ^{13}C or ^{14}C is used as a tracer for newly fixed carbon, the rate of synthesis for each compound can be calculated from the amount of tracer in each compound (MAAs and xanthophyll pigments). The newly synthesized compounds have specific activities that equal the specific activity of the inorganic carbon (Goericke & Welschmeyer 1993, Ha et al. 2012).

In the present study, the photoprotective strategy of the diatom *Porosira glacialis* (Grunow) Jørgensen, which lives in polar oceans, was investigated by incubating cells of *P. glacialis* with labeled carbon tracers under indoor UV exposure. The synthesis rates of photoprotective UV-absorbing compounds (MAAs) and xanthophyll pigments were determined as a function of the duration of exposure to artificial UVR. In addition, the initial productivity of photoprotective compounds was used as an indicator of the survival ability of phytoplankton adapted to extreme environments. In this study, the net production rate of each compound was determined using a ^{13}C tracer. This experimental approach provided insight into the real-time processes of delivery and distribution of UV-absorbing compounds in diatom cells in response to UVR.

Materials and methods

Porosira glacialis (KCCPM serial number AnM0008) is a dominant phytoplankton species in polar waters. The cultures used were provided by the Korea Polar Research Institute (KOPRI) culture collections for polar microorganisms (KCCPM). Stock cultures were grown under a light intensity of 30 $\mu mol\, m^{-2}\, s^{-1}$ and a temperature of 4°C. The salinity of the culture solution was 32–34%. *Pororsira glacialis* was sub-cultured under a light intensity of 30 $\mu mol\, m^{-2}\, s^{-1}$. Prior to the exposure tests, the last sub-culture was grown under a light intensity of 15–20 $\mu mol\, m^{-2}\, s^{-1}$. Ultraviolet-A (UVA) and ultraviolet-B (UVB) irradiation were provided by TL-D 15 W and Ultraviolet-B Actionic BL 15 W lamps (Philips, Eindhoven, The Netherlands), respectively. The source of visible light was an FL 15D lamp (15 W, Kumho Electric, Seoul, Korea). Diatom samples were transferred to culture media and kept in darkness for about 24 h for adaptation prior to exposure experiments.

A unialgal culture of *P. glacialis* was grown in f/2 medium (Guillard & Ryther 1962) prepared from filtered Antarctic seawater. Incubations were performed in 500 mL, UV-transparent quartz bottles. The bottles were covered with two types of UV cut-off filters. The first was a 295 nm cut-off filter (Ultraphan, UV Opak, Digefra, Munich, Germany) that transmits UVB radiation, UVA-A radiation, and photosynthetically active radiation (PAR).

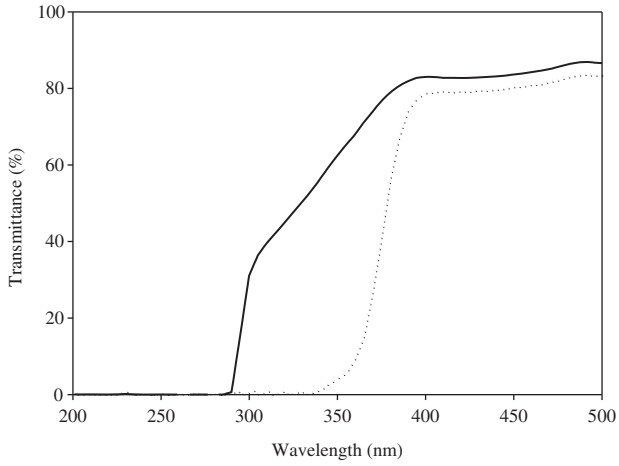

Fig. 1. Transmittance spectra of the quartz bottles used for growing *P. glacialis* and the cut-off filters (solid line = 295-nm cut-off filter, broken line = 395-nm cut-off filter) used to cover the PAR, and the UVA and UVB lamps respectively.

Combined PAR + UVA + UVB is designated UVR. The second was a 395nm cut-off filter (Ultraphan, UV Opak, Digefra) that transmits only PAR (Fig. 1). The intensity of UVR was examined under the following conditions: 5.2 $\mu W\, m^{-2}$ at 250 nm (UVB); 12.3 $\mu W\, m^{-2}$ at 320 nm (UVA); and 1.8 $\mu W\, m^{-2}$ at 395 nm (PAR) as measured with a UVX®radiometer (model UVX-25 and UVX-31, UVP, Upland, CA, USA). UV exposure tests were conducted continuously for 3 days at 4°C. To determine the levels of chlorophyll *a* (Chl *a*), MAAs and xanthophyll pigments, and carbon fixation rate, sample aliquots were collected at 24 h intervals. Culture bottles were mixed thoroughly prior to removing the sample aliquots.

Carbon fixation rate

To determine the rate of carbon fixation due to photosynthesis, $NaH^{13}CO_3$ (98% ^{13}C) was added to the seawater samples. To increase the isotopic ratio of particulate organic carbon, the ^{13}C level was increased to 10% in the dissolved inorganic carbon (DIC) pool. 10 mL of each sample was then filtered through pre-baked (450°C, 4 h) GF/F 25-mm filter paper and stored at –80°C until analysis. The filtered samples were dried completely in a lyophilizer and exposed to 1N HCl fumes overnight to remove inorganic carbon. The samples were then neutralized with NaOH fumes. The degree of ^{13}C enrichment was measured using an EA-irMS (EuroEA-Isoprime IRMS, GV Instruments, Manchester, UK) and the carbon fixation rate was calculated using the expression developed by Hama et al. (1983).

$$\text{Carbon uptake rate}(\rho c(t)) = \frac{\Delta \text{POC(t)}}{t} = \frac{\alpha_{is} - \alpha_{ns}}{\alpha_{ic} - \alpha_{ns}} \times \frac{\text{POC(t)}}{t} \quad (1)$$

a_{is}: the ^{13}C % of particulate organic carbon in an incubated sample;

a_{ns}: the ^{13}C % of particulate organic carbon in a natural (non-incubated) sample;

a_{ic}: the ^{13}C % of dissolved inorganic carbon in the incubation bottle;

t: incubation time;

POC(t): concentration of particulate organic carbon in the incubated sample.

Extraction and analysis of MAAs and pigments

To determine MAAs in particulate organic matter, 50 mL of each sample was filtered through pre-baked GF/F 47 mm filter paper and stored at –80°C until analysis. Three milliliters of 100% MeOH was added to each filtered sample, which was then sonicated for 30 s in an ultrasonicator (30 s, 50 W; ULH-700 s, Ulsso Hitech, Chungcheongbuk-do, Korea) to break down the sample physically. Samples were refrigerated at 4°C overnight and then extracted. After extraction, a 0.2 μm syringe filter (PTFE 0.20 μm hydrophobic, Millipore, Billerica, MA, USA) was used to transfer the samples into 2mL microtubes. A centrifugal evaporator (CVE-200D, EYELA, Tokyo, Japan) was used to dry each sample completely. The dried samples were then dissolved in 500 μL of distilled water. To this was added 100 μ L of chloroform and the samples were centrifuged for 10 min at 10,000 rpm. A total of 400 μ L of supernatant was removed and injected into a high-performance liquid chromatography column (HPLC) to quantify the MAAs in each sample.

To determine pigment composition, phytoplankton samples (50 mL) were filtered over pre- combusted 25 mm GF/F filters. The filter papers were placed in a Petri dish wrapped with aluminum foil to prevent photolysis during storage at –80°C. To extract the pigments, filter papers were placed in Teflon bottles containing 100% acetone (3 mL). Prior to extraction, 50 μ L of 1 mg mL^{-1} apo-8-carotennoate was added to each sample as an internal standard. Pigment extraction was performed with an ultrasonicator (30 s, 50 W; ULH-700 s, Ulsso Hitech) and samples were stored for 24 h at 4°C. One milliliter of the extract was passed through a syringe filter (PTFE 0.2 μm hydrophobic) to remove any debris. Quantitative pigment analyses were performed by HPLC.

MAA analyses were performed with an HPLC system (1200 series, Agilent Technologies, San Jose, CA, USA; columns: Zorbax Eclipse XDB C18 column, 5 μm, 150 × 4.6 mm, Agilent Technologies). The detector was an Agilent DAD (G1315D) and absorbance was measured at 313 nm (250–750 nm scan). MAA compounds [shinorine (SH) and porphyra-334 (PR)] were collected individually using a fraction collector [Agilent analyte (G1364C) FC] (Fig. 2a). The mobile phase consisted of 100% distilled water (with 0.1% acetic acid) at a constant flow of 0.8 mL min^{-1}. Shinorine and porphyra-334 were used as standard reference compounds for quantitative MAA analyses. The HPLC method used for accessory pigment analyses was based on that of Jeffrey & Wright (1997). Pigment compounds were separated through an HPLC column (Zorbax Eclipse XDB C18 column, 250 × 4.6 mm, 5 μm) with mobile phase A (80:20 methanol:0.5 M ammonium acetate, pH 7.2, v/v), mobile phase B (90:10 acetonitrile:deionized water, v/v) and mobile phase C (100% ethyl acetate). A segmented linear gradient was programmed as follows. Initial conditions were re-established by a reversed linear gradient (10 min). The flow rate was 1 mL min^{-1} and the sample injection volume was 100 μ L. The individual absorbance of each compound was detected at 430 nm (250–750 nm scan). The identification of peaks was based on the retention time of pigment standards (DHI Water & Environment, Hørsholm, Denmark) (Fig. 2b). Pigment concentrations were calculated based on chromatographic peak areas in accordance with the method developed by Park (2006). Analytical results were processed with an Agilent HPLC 1200 series ChemStation integrator-processor.

Calculated net production and turnover rates of MAAs

MAA and pigments were collected through a tin cap (including the pre-baked filter paper). After solvent removal by centrifugal evaporation (CVE-200D, EYELA), the ^{13}C content of each compound was measured using EA-irMS (EuroEA-Isoprinme IRMS, GV Instruments). The net production rate of each MAA and pigment (specific compound net production rate, SPR) was calculated from the compound concentration and the atomic percentage of ^{13}C, using the modified equation proposed by Ha et al. (2012) (Hama & Handa 1987, Hama et al. 1988, Falkowski 1991, Takahashi et al. 1991).

$$\Delta \mathrm{SPR(t)} = \mathrm{SPR} \times \frac{\alpha_{is} - \alpha_{ns}}{\alpha_{ic} - \alpha_{ns}} \tag{2}$$

Δ SPR(t): The amount of each specific carbon compound produced photosynthetically during incubation;

a_{is}: The atomic percentage of ^{13}C in each of the specific compounds in the incubated sample;

a_{ns}: The atomic percentage of ^{13}C in each specific compound in the natural sample;

a_{ic}: The atomic percentage of ^{13}C in samples incubated in ^{13}C-enriched medium;

SPR: Concentration of each specific carbon compound at the end of incubation;

The turnover rate of each MAA can also be calculated using the following equation to understand the relationship between MAA concentration and net production rate (Hama et al. 1983).

$$\mathit{Turnover\ rate}(\mathrm{t}) = \frac{\alpha_{is} - \alpha_{ns}}{\alpha_{ic} - \alpha_{ns}} \times \frac{1}{t} \tag{3}$$

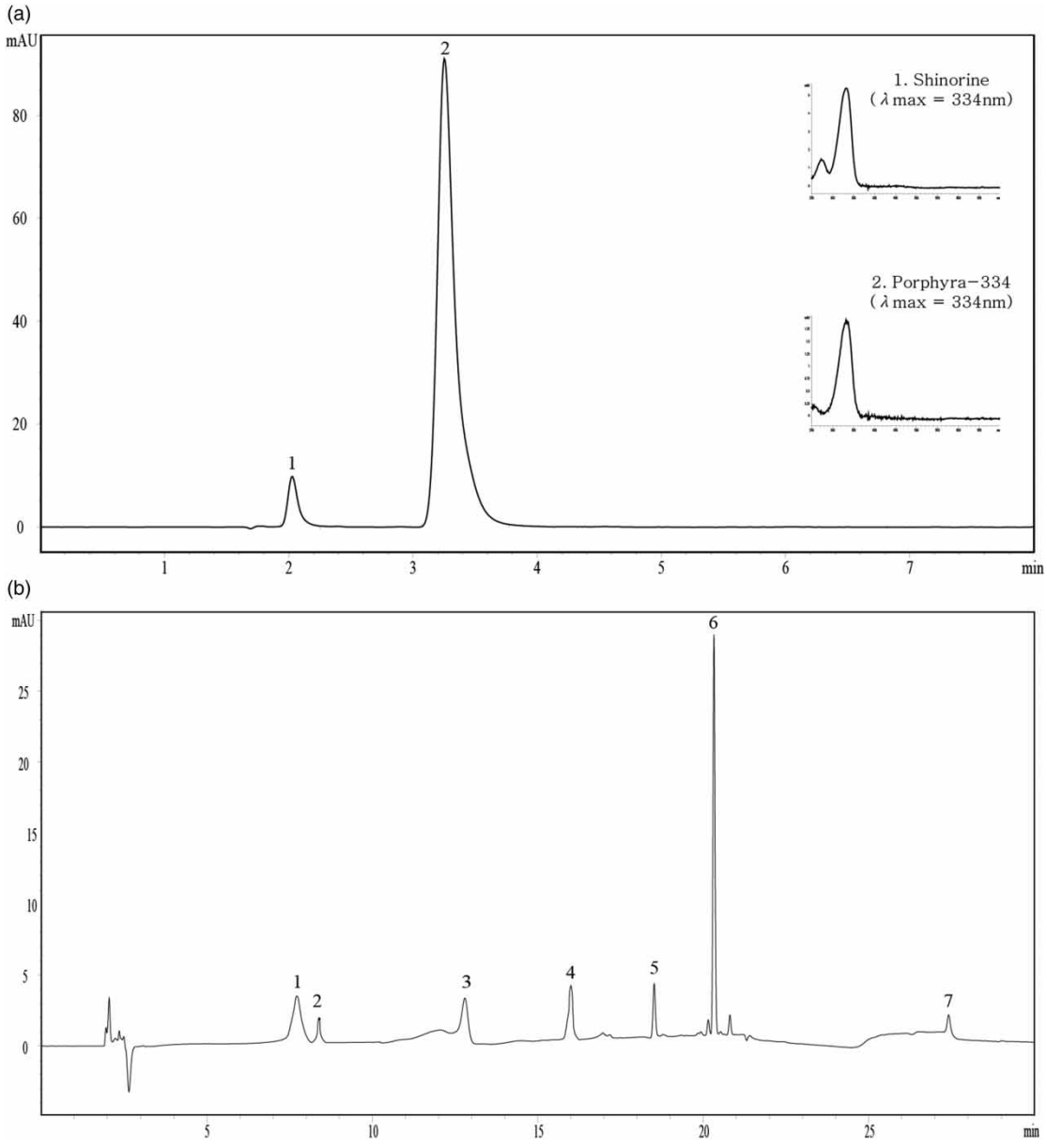

Fig. 2. An HPLC chromatogram shows the (a) MAA and (b) pigment composition (b) of *P. glacialis* cells. (a) 1 = shinorine, 2 = porphyra-334; (b) 1 = chlorophyll c3; 2 = chlorophyll c2; 3 = fucoxanthin; 4 = diadinoxanthin; 5 = cantaxanthin; 6 = chlorophyll *a*; 7 = β-carotene.

Possible isotopic discrimination against ^{13}C during photosynthetic uptake was not considered in this study because of its negligible effect on the uptake rate (Hama et al. 1983).

Statistical analyses

All measurements were made in triplicate on different cultures and the results are expressed as means with a single standard deviation. Statistical differences between the results were tested using RM-ANOVAs (version 18, SPSS Inc., Chicago, IL, USA) with time as the repeated factor. Data from each individual time were also analyzed with *t*-tests, and *P* values of < 0.05 and < 0.01 indicated statistically significant differences.

Results

Growth and carbon uptake rates and MAA concentrations in P. glacialis

Significant differences (RM-ANOVA $F = 1096.8$, $P < 0.01$) were observed in the carbon uptake rates and MAA concentrations in *P. glacialis* cells that were continuously exposed to either PAR or UVR for 72 h. The carbon uptake rate under continuous exposure to PAR for 24 h was 0.54 ($\pm$0.05) mgC L^{-1} d^{-1}. In contrast, exposure to UVR

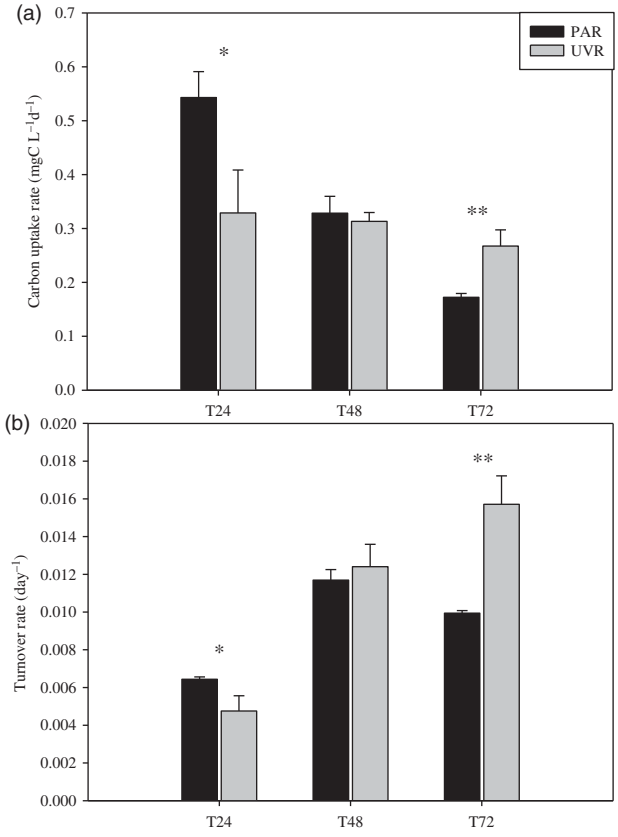

Fig. 3. (a) Carbon uptake rate and (b) turnover rate of *P. glacialis* as a function of PAR and UVR exposure. Black bar = PAR incubation; Gray bar = UVR incubation. *P* values are indicated by asterisks: *,< 0.05 and **, < 0.01.

for the same period yielded 0.33 (±0.08) mgC L^{-1} d^{-1}. However, after 72 h, this rate dropped to 0.17 (±0.01) mgC L L^{-1} d^{-1}, lower than both the initial carbon uptake rate of *P. glacialis* exposed to PAR and that exposed to UVR (0.27 (±0.03) mgC L^{-1} d^{-1}) (Fig. 3). After 24 h of exposure, the growth rates were 7.02 (±0.85) and 7.85 (±0.17), exposed to PAR and UVR respectively. However, after 72 h of exposure, these values were 7.26 (±4.57) and 13.84 (±6.10) respectively, representing a significant increase in the growth rate for cells exposed to UVR (Table 1). The Chl *a* concentration was 10.94 µg L^{-1} prior to light exposure (T0) and reached a maximum of 14.66 (±0.37) µg L^{-1} after 24 h of PAR exposure. However, the Chl *a* concentration fell to 13.28 (±0.8) µg L^{-1} after 72 h of PAR exposure. In cells exposed to UVR, the Chl *a*concentration fell to 13.28 (±0.8) µg L^{-1} after reaching a maximum of 15.18 (±0.07) µg L^{-1} (Table 1).

The concentrations of both DD and MAAs tended to increase with exposure time (Table 1). The ratio of DD to Chl *a*, a xanthophyll compound, was initially 0.33 increasing to 0.58 after 24 h of PAR exposure, and to a maximum of 0.83 after 72 h. In cells exposed to UVR, a maximum DD:Chl *a* ratio of 0.88 was reached from an initial value of 0.58 (Table 1). Such characteristics were observed with

Table 1. Concentration of each protective compound, chl *a*, and growth rate of *P. glacialis* during exposure to artificial UV radiation.

	Initial	PAR	UVR
Chl *a* (mg/L)			
T0	10.94		
T24		14.66 (±0.37)	15.18 (±0.07)
T48		14.13 (±0.76)	12.97 (±0.14)
T72		12.11 (±0.54)	13.28 (±0.8)
Growth rate			
T24		7.02 (±0.85)	7.85 (±0.17)
T48		12.22 (±3.67)	8.18 (±0.74)
T72		7.26 (±4.57)	13.84 (±6.1)
Diadinoxanthin (ratio of chl *a*)			
T0	0.33		
T24		0.58 (±0.02)	0.58 (±0.03)
T48		0.69 (±0.003)	0.78 (±0.02)
T72		0.83 (±0.01)	0.88 (±0.02)
Shinorine (µg/µg chl *a*)			
T0	0.65 (±0.11)		
T24		0.39 (±0.003)	0.37 (±0.01)
T48		0.41 (±0.02)	0.45 (±0.03)
T72		0.42 (±0.003)	0.43 (±0.004)
Porphyra-334 (µg/µg chl *a*)			
T0	5.84 (±0.4)		
T24		4.78 (±0.04)	4.60 (±0.12)
T48		5.16 (±0.31)	4.78 (±0.27)
T72		4.90 (±0.06)	5.26 (±0.35)

UV-absorbing compounds such as shinorine and porphyra-334. The concentration of light-scattering compounds, such as DD, per unit Chl *a* decreased when *P. glacialis* was first exposed to light, but then tended to increase with increased exposure time. Shinorine concentration per unit Chl *a* was initially 0.65 (±0.11) µ g mg Chl a^{-1}, but increased from 0.37 (±0.01) to 0.43 (±0.004) µ g mg Chl a^{-1} (maximum) after exposure to UVR. The initial concentration of porphyra-334 (5.84 ± 0.4 µg mg Chl a^{-1}) was higher than that of shinorine. After exposure to UVR, this increased from 4.6 (±0.12) to 5.26 (±0.35) µ g mg Chl a^{-1} (maximum) (Table 1).

Net production rate of MAAs in P. glacialis

The net production and turnover rates of Chl *a* and DD in P. *glacialis* showed similar trends with incubation time (Fig. 4). After 24 h exposure, the net production rates of Chl *a* and DD under UVR were significantly higher (10.1 ± 0.52 fg C L^{-1} d^{-1} and 6.6 ± 0.4 fg C L^{-1} d^{-1} respectively) than those under PAR (7.9 ± 0.2 fg C L^{-1} d^{-1} and 5.3 ± 0.5 fg C L^{-1} d^{-1} respectively). However, the net production rates of Chl *a* and DD decreased with prolonged UVR exposure. Net production and turnover rates of both Chl *a* and DD were higher when cells were exposed to PAR compared to UVR (Fig. 4).

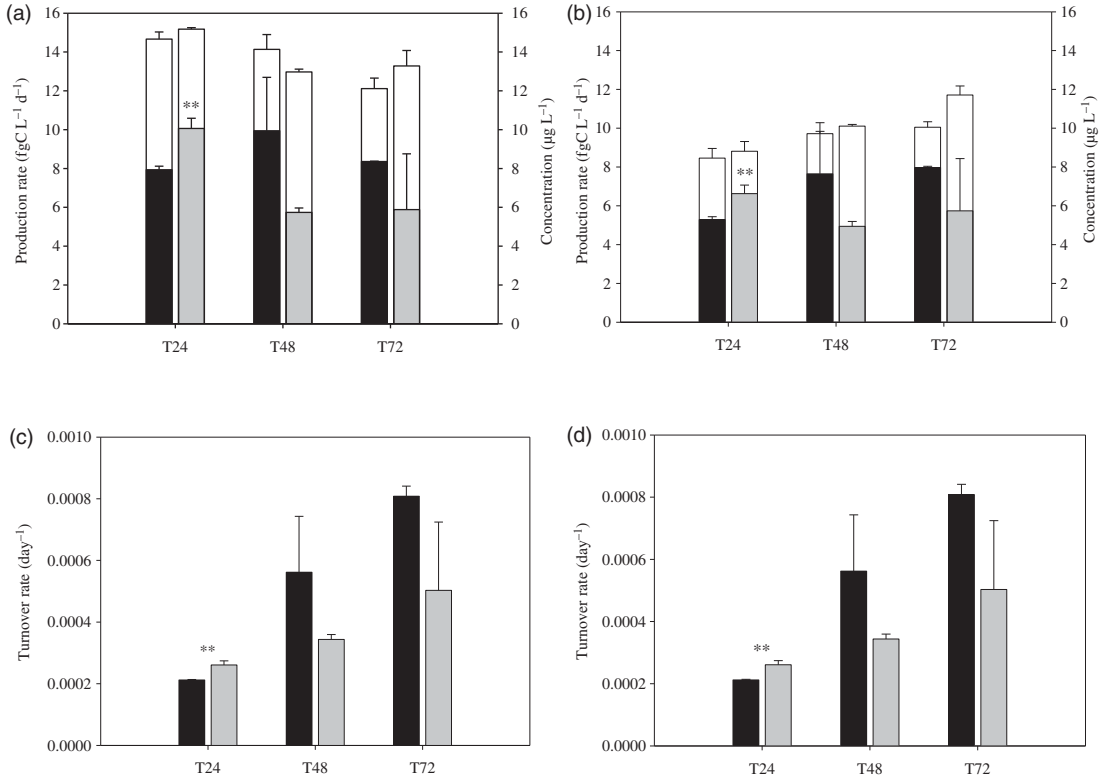

Fig. 4. The (a, b) net production rate and (c, d) turnover rate of (a, c) chlorophyll *a* and (b, d) diadinoxanthin in *P. glacialis* as a function of PAR and UVR exposure conditions. The white bars indicate the absolute values of each compound concentration (a, b). Black bars indicate PAR exposure and gray bars correspond to UVR exposure. *P* value is given by **, which indicates < 0.01.

The UV-absorbing compounds shinorine and porphyra-334 showed a different trend with exposure compared to DD, a xanthophyll (Fig. 5). After 72 h of exposure, the net production rate of the UV-absorbing compounds was higher in *P. glacialis* exposed to UVR than it was with PAR. Regardless of exposure time, the net production rate of UV-absorbing compounds tended to decrease with increased exposure time. After 24 h of exposure, the net production rate of shinorine in cells under PAR ($0.15 \pm 0.001\ \mu g\ C\ L^{-1}\ d^{-1}$) was similar to that under UVR ($0.15 \pm 0.01\ \mu g\ C\ L^{-1}\ d^{-1}$). However, after 72 h of exposure, the production rates of shinorine were higher under UVR ($0.09 \pm 0.02\ \mu g\ C\ L^{-1}\ d^{-1}$) than under PAR ($0.05 \pm 0.003\ \mu g\ C\ L^{-1}\ d^{-1}4$). The net production rate of shinorine did not differ significantly with respect to exposure time and light conditions ($F = 6.9$, $P = 0.05$). In contrast, the net production rate of porphyra-334 differed significantly with these factors ($F = 11.31$, $P < 0.05$). The change in production rate of porphyra-334 was similar to that of shinorine but values were consistently lower. In *P. glacialis* exposed to UVR, carbon uptake into shinorine tended to be faster and proportional to exposure time. Rapid growth was observed after 72 h under PAR (Fig. 5). However, the turnover rate of porphyra-334 was less than one-tenth that of shinorine. In addition, despite higher concentrations, both the turnover rate and net production rate of porphyra-334 were lower than those of shinorine (Fig. 5).

Effects of UVR exposure

Significant changes (determined by RM-ANOVA) were observed in growth rates and Chl *a* concentrations as a result of exposure to UVR. Carbon uptake rate and net porphyra-334 production rate depended on the type of exposure (UVR or PAR) and the duration of exposure (Table 2). UVR treatments had no effect on the concentrations of shinorine or porphyra-334, or on the net production rate of shinorine. The fact that no statistical differences were observed in the net production rate of shinorine suggests active stimulation of shinorine in *P. glacialis* cells. The net production rate of porphyra-334 depended on the duration of UVR exposure (Table 2).

Discussion

Porosira glacialis is associated with cold coastal waters adjacent to sea ice (Hasle & Heimdal 1968, Taylor et al. 1997, Zielinski & Gersonde 1997). It grows predominantly in the open ocean beyond the sea ice edge (Zielinski & Gersonde 1997) and adopts an effective photoprotective strategy against exposure to UVB by exploiting UV-absorbing compounds such as shinorine and phophyra-334 (Riegger & Robinson 1997, Sinha et al. 2007). Our results show adaptations for UV tolerance, revealed by changes in growth rate and Chl *a* concentration under UV exposure. Zudaire & Roy (2001) reported that *T. weissflogii* tolerates long-

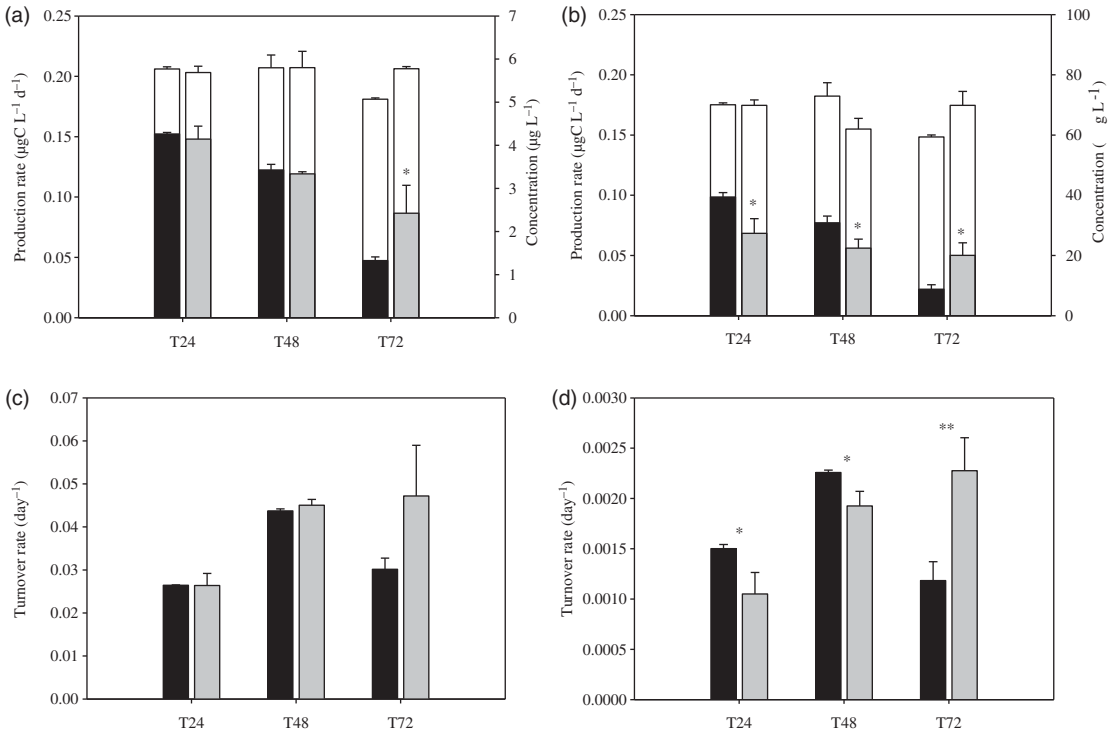

Fig. 5. The net production rates (a, b) and turnover rates (c, d) of (a, c) shinorine and (b, d) porphyra-334 in *P. glacialis* are given as a function of PAR and UVR exposure. White bars indicate the absolute levels of each compound (a, b). Black and gray bars indicate PAR and UVR exposure respectively. *P* values =*, < 0.05 and **, < 0.01.

Table 2. Results of repeated-measures analysis of variance of the effects of the UVR treatments.

	UV treatment	time	UVR × time
Growth rate	486.99**	2.162	28.45**
Chl a concentration	150.72**	21.03**	13.42*
DD	88.74*	522.56**	4.44
SH	1.19	75.45**	3.1
PR	1.74	9.13*	1.78
Carbon uptake rate	3.98	25.79**	1096.82**
PP of DD	1.39	0.38	12.24*
Turnover rate of DD	3.63	14.13*	6.74
PP of SH	3.00	284.27**	6.90
PP of PR	5.49	226.21**	11.32*
Turnover rate of SH	3.01	54.67**	5.25
Turnover rate of PR	0.82	78.51**	18.60**

Values are F statistics for 3 replicate treatments. Chl a = chlorophyll a; DD = diadinoxanthin; SH = shinorine; PR = porphyra-334; PP = production rate; UVR = the between-group factor; Time = the within-group factor; UVR × times = the interaction between UVR treatment and Time.
*$P < 0.05$.
**$P < 0.01$

term (40 days) UVB radiation. This contrasts with other diatoms, such as *Phaeodactylum tricornutum* (Behrenfeld et al. 1992), or *Thalassiosira nordenskioldii*, *Nitzschia closterium*, and *Cyclotella* sp. (Buma et al. 1996), in which decreased growth rates were observed. Rech et al. (2005) showed that the growth rate of *Amphora coffeaeformis* was reduced by about 18% by various long-term UVB treatments, and Fouqueray et al. (2007) reported that its growth rate was 20% lower than the control after between 3 and 5 days UV exposure.

The current study explored the effects of PAR and UVR exposure on *P. glacialis* in terms of Chl *a* concentration and growth rate (Table 1). Under these conditions and in all cases, the carbon uptake rate dropped as the physiological activity of the organism steadily weakened. During the first 48 h of growth, cells were more physiologically active under UVR than PAR (Fig. 3). However, after 72 h of exposure to artificial UVR, the carbon uptake rate was higher than under PAR exposure. This decrease in carbon uptake rate is likely related to the initial decrease in photochemical capacity, an indicator of photoinhibition, as well as to the potential metabolic cost of initially defending against UV-related damage (Hazzard et al. 1997, Zudaire & Roy 2001). Previous studies have shown that UVR influences the productivity of phytoplankton and carbon and nutrient uptake rates (Behrenfeld et al. 1995, Helbling et al. 1996, Wängberg et al. 2006). The results of our study show that phytoplankton can live successfully in an extreme environment by responding to, and controlling, strong light and UVR through the production of photoprotective compounds (Moeller et al. 2005).

The high concentration of the MAAs in *P. glacialis* demonstrated the maintenance of carbon uptake through the

manipulation of photoprotective compounds (Table 1). The compound-specific stable isotope study allowed the production rates of newly synthesized MAAs to be calculated. The results of these calculations provided additional evidence for the protective role played specifically by newly synthesized MAAs, rather than by pre-existing MAAs in the cells (Fig. 5). Note that the rate of MAA production in response to an external stress (UVR) appears to be a defensive strategy since it increases despite a reduction in the carbon uptake rate. The results of the current study showed that the carbon uptake ability of phytoplankton exposed to UVR is greater than that of phytoplankton exposed to PAR. This is possible through the maintenance of a high MAA content within the cell and the continued production of MAAs despite the relatively poor biological condition of the phytoplankton cells themselves, as a result of UVR exposure. MAAs are located in the cytoplasm and are not coupled directly to the cellular photosystems (Moisan & Mitchell 2001). As such, they act as a passive sunscreen (Garcia-Pichel & Castenholz 1993). Exposure to UVR results in a positive correlation between the carbon fixation rate and MAA concentration in the natural phytoplankton community, which suggests effective photoprotection (Shick et al. 1991, Dunlap et al. 1995, Helbling et al. 1996, Neals et al. 1998). Several studies on natural populations have suggested that MAA induction is related to irradiance (Shick et al. 1991, Karentz 1994). Vernet et al. (1994) observed that UV absorption in Antarctic phytoplankton, presumably due to MAAs, was higher in surface waters and decreased with depth.

The two MAAs (shinorine and porphyra-334) synthesized by *P. glacialis* responded differently with respect to net production rate v. exposure time. Concentrations of porphyra-334 were higher than those of shinorine, even though the net production rate of porphyra-334 was lower. Marine diatoms and cyanobacteria have been shown to produce both porphyra-334 and shinorine upon UV irradiation (Helbling et al. 1996, Sinha et al. 2003, Klisch & Häder 2008). A common bloom-forming cyanobacterium was able to synthesize an MAA that directly absorbed UVR (Sinha et al. 2003). However, in *P. glacialis* the net production rate of shinorine was higher than that of porphyra-334, which was present at higher concentrations. Under natural solar radiation, increasing concentrations of shinorine, a bisubstituted MAA containing both glycine and serine, with an absorption maximum at 334 nm (Sinha et al. 2001), were only found during light periods (Sinha et al. 2001, Mushir & Fatma 2011). UVR enhances the production of shinorine (Portwich & Garcia-Pichel 1999), and Karsten et al. (1998a) reported that shinorine synthesis was specifically induced by the exposure to UVA radiation. Shinorine is the most common MAA found in macroalgae, and has been found in species collected from tropical to Arctic waters (Banazak et al. 1998, Karsten et al. 1998b, Franklin et al. 2001). Shinorine is also the most rapidly accumulated compound synthesized in *Stylophora* colonies when they are exposed to UVR under controlled laboratory conditions (Shick et al. 1999).

The other reason for the increased carbon uptake rate of *P. glacialis* exposed to UVR rather than PAR is the synthesis of xanthophyll compounds. The net production rate of DD, a photoprotective xanthophyll pigment, was nearly constant as a function of exposure time. However, the productivity of DD was higher under UVR than under PAR after 24 h of culture incubation (Fig. 4). The photoprotective pigment DD has been reported in the Prymnesiophyta, Dinophyta, and Bacillariophyta (Laviale & Neveux 2011). In diatoms, the one-step xanthophyll cycle (de-epoxidation of DD to diatoxanthin, DT) and the associated light-induced increase in DT are known to contribute to photoprotection (Moisan et al. 1998, Demming-Adams et al. 1999). Although some studies have reported UVB-induced damage to this xanthophylls cycle (Pfündel et al. 1992), others have observed an increase in DD and DT concentrations in some UVB-exposed diatoms and prymnesiophytes (Buma et al. 1996, Buma et al. 2000).

Many phytoplankton species adopt a complementary strategy of producing photoprotective pigments that are also UV-absorbing compounds (Ha et al. 2010). MAAs and photoprotective pigments both act to eliminate light energy (Sinha & Häder 2002). Such a complementary relationship is known to be an adaptive strategy and is tailored according to the type of phytoplankton or specific environmental factors (Ha et al. 2010, Korbee et al. 2010). Korbee et al. (2010) showed that the accumulation of MAA by *Heterocapsa* sp. (Dinophyta) increases as a result of the conversion of excess energy from UVR to heat in the presence of excess nitrogen (Conde et al. 2004). The MAA content of the cells decreases if nitrogen is limited, but the de-epoxidation of excess energy increases through the effects of the pigments in the xanthophyll cycle. In addition, a study conducted by Ha et al. (2010) on an indoor culture of *Phaeocytis* sp. showed that changes in the concentrations of β-carotene and DD depend on the duration of UVR exposure. Furthermore, the concentration of MAAs increases proportionally with exposure time to artificial UVR (Ha et al. 2010). Zudaire & Roy (2001) reported that photoprotection first arose through an increase in levels of xanthophyll cycle carotenoids, but was then replaced by an increase in UV-absorbing MAAs. The fact that elevated net production rates of DD were not maintained after the increase in net production rate of MAAs suggests that MAAs served to protect against photoinhibition, enabling a subsequent decrease in the photoprotective xanthophyll cycle pigments.

The results of this study shed light on the synthetic pathways of photoprotective compounds and the carbon cycle within *P. glacialis*. In particular, the contrasting patterns that define the production of photoprotective pigments and MAAs as a function of time and UV exposure were examined in detail. Complementary changes in the production rate of MAAs and xanthophyll pigments with exposure time

are the direct result of the allocation of carbon to different photoprotective compounds. The results of this study show that organic carbon is initially fixed to produce photoprotective pigments and that carbon (as determined by ^{13}C tracer experiments) is fixed to produce MAAs within the cell after a particular length of exposure.

This study reveals the selective strategies adopted in response to a hazardous stress in the stationary phase of phytoplankton growth. The exposure of *P. glacialis* to UVR allowed the net production rate of newly synthesized photoprotective pigments and UV-absorbing compounds with photoprotective roles to be calculated. According to the physiological condition of the cells, the carbon uptake ability of *P. glacialis* shows a close relationship with the production of photoprotective compounds.

Acknowledgements

We thank Y.N. Kim for providing assistance in laboratory work. This work was supported by the Korea Polar Research Institute projects (PM12020).

References

Banazak A.T., Lesser M.P., Kuffner I.B. & Ondrusek M. 1998. Relationship between ultraviolet (UV) radiation and mycosporine-like amino acids (MAAs) in marine organisms. *Bulletin of Marine Science* 63: 617–628.

Behrenfeld M.J., Hardy J.T. & Lee II H. 1992. Chronic effects of ultraviolet-B radiation on growth and cell volume of *Phaeodactylum tricornutum* (Bacillariophyceae). *Journal of Phycology* 28: 757–760.

Behrenfeld M.J., Lean D.R.S. & Lee II H. 1995. Ultraviolet-B radiation effects on inorganic nitrogen uptake by natural assemblages of oceanic plankton. *Journal of Phycology* 31: 25–36.

Buma A.G.J., Zemmelink H.J., Sjollema K. & Gieskes W.W.C. 1996. UVB radiation modifies protein and photosynthetic pigment content, volume and ultrastructure of marine diatoms. *Marine Ecology Progress Series* 142: 47–54.

Buma A.G.J., Van Oijen T., Van De Poll W., Veldhuis M.J.W. & Gieskes W.W.C. 2000. The sensitivity of *Emiliania huxleyi* (Prymnesiophyceae) to ultraviolet-B radiation. *Journal of Phycology* 36: 296–303.

Conde F., Churio M. & Previtali C. 2004. The deactivation pathways of the excited-states of the mycosporine-like amino acids shinorine and porphyra-334 in aqueous solution. *Photochemiscal & Photobiological Sciences* 3: 960–967.

Demming-Adams B. & Adams W. 1996. The role of xanthophyll cycle carotenoids in the protection of photosynthesis. *Trends in Plant Science* 1: 21–26.

Demming-Adams B., Adams III W.W., Eddert V. & Logan B.A. 1999. Ecophysiology of the xanthophyll cycle. In: *The photochemistry of carotenoids* (Eds. by H.A. Frank, J.J. Young, G. Britton, & R.J. Cogdell), pp. 245–239. Kluwer, Dordrecht.

Dunlap W.C., Rae G.A., Helbling E.W., Villafañe V.E. & Holm-Hansen O. 1995. Ultraviolet-absorbing compounds in natural assemblages of antarctic phytoplankton. *Antarctic Journal of the United States* 30: 323–326.

Falkowski P.G. 1991. Species variability in the fractionation of ^{13}C and ^{12}C by marine phytoplankton. *Journal of Plankton Research* 13: 21–28.

Fouqueray M., Mouget J.L., Morant-Manceau A. & Trmblin G. 2007. Dynamics of short-term acclimation to UV radiation in marine diatoms. *Journal of Photochemistry and Photobiology B: Biology* 89: 1–8.

Franklin L.A., Kräbs G. & Kuhlenkamp R. 2001. Blue light and UV-A radiation control the synthesis of mycosporine-like amino acids in *Chondrus crispus* (Florideophyceae). *Journal of Phycology* 37: 257–270.

Garcia-Pichel F. & Castenholz R.W. 1993. Occurrence of UV-absorbing, mycosporine-like compounds among cyanobacterial isolates and an estimate of their screening capacity. *Applied and Environmental Microbiology* 59: 163–169.

Goericke R. & Welschmeyer N.A. 1993. The chlorophyll-labeling method: Measuring specific rates of chlorophyll *a* synthesis in cultures and in the open ocean. *Limnology and Oceanography* 38: 80–95.

Guillard R.R.L. & Ryther J.H. 1962. Studies of marine planktonic diatoms. I. *Cyclotella nana* Hustedt, and *Detonula confervacea* (Cleve) Gran. *Canadian Journal of Microbiology* 8: 229–239.

Ha S., Kang S., Park M., Kim Y., Kang S. & Shin K. 2010. Photoinduction of UV-absorbing compounds and photoprotective pigment in *Phaeocystis pouchetii* and *Porosira glacialis* by UV exposure. *Ocean and Polar Research* 32: 397–409.

Ha S., Kim Y., Park M., Kang S., Kim H. & Shin K. 2012. Production of mycosporine-like amino acids of *in situ* phytoplankton community in Kongsfjorden, Svalbard, Arctic. *Journanl of Photochemistry and Photobiology B: Biology* 114: 1–14.

Häder D.P., Kumar H.D., Smith R.C. & Worrest R.C. 2007. Effects of solar UV radiation on aquatic ecosystems and interactions with climate change. *Photochemiscal & Photobiological Sciences* 6: 267–285.

Hama T. & Handa N. 1987. Pattern of organic matter production by natural phytoplankton population in an eutrophic lake: 1. *Intracellular products. Archiv für Hydrobiologie* 109: 107–120.

Hama T., Handa N., Takahashi M., Whitney F. & Wong F.C.S. 1988. Change in distribution patterns of photosynthetically incorporated C during phytoplankton bloom in controlled experimental ecosystem. *Journal of Experimental Marine Biology and Ecology* 120: 39–56.

Hama T., Miyazaki T., Ogawa Y., Iwakuma T., Takahashi M., Otsuki A. & Ichimura S. 1983. Measurement of photosynthestic production of a marine phytoplankton population using a stable isotope. *Marine Biology* 73: 31–36.

Hasle G.R. & Heimdal B.R. 1968. Morphology and distribution of the marine centric diatom *Thalassiosira antarctica* Comber. *Journal of the Royal Microscopical Society* 88: 357–369.

Hazzard C., Lesser M.P. & Kinzie III R.A. 1997. Effects of ultraviolet radiation on photosynthesis in the subtropical marine diatom, *Chaetoceros gracilis* (Bacillariophyceae). *Journal of Phycology* 33: 960–968.

Helbling E.W., Villafañe V., Ferrario M. & Holm-Hansen O. 1992. Impact of natural ultraviolet radiation on rates of photosynthesis and on specific marine phytoplankton species. *Marine Ecology Progress Series* 80: 89–100.

Helbling E.W., Chalker B.E., Dunlap W.C., Holm-Hansen O. & Villafañe V.E. 1996. Photoacclimation of antarctic marine diatoms to solar ultraviolet radiation. *Journal of Experimental Marine Biology and Ecology* 204: 85–101.

Jeffrey S.W. & Wright S.W. 1997. Qualitative and quantitative HPLC analysis of SCOR reference algal cultures. In: *Phytoplankton pigments in oceanography: guidelines to modern methods, vol. 10*. (Eds. by S.W. Jeffrey, R.F.C. Montoura & S.W. Wright), pp. 343–360. UNESCO Monographs on Oceanographic Methodology, Paris.

Karentz D. 1994. Ultraviolet tolerance mechanisms in Antarctic marine organisms, in Ultraviolet radiation in Antarctica: measuremnets and biological effects. *Antarctic Research Series* 62: 93–110.

Karentz D. 2001. Chemical defenses of marine organisms against solar radiation exposure: UV-absorbing mycosporine-like amino acids and scytonemin. In: *Marine chemical ecology* (Eds. by J.B. McClintock & B.J. Baker), pp. 481–520. CRC Press, Boca Raton, Florida, USA.

Karentz D., Cleaver J.E. & Mitchell D.L. 1991. Cell survival characteristics and molecular responses of Antarctic phytoplankton to ultraviolet-B radiation. *Journal of Phycology* 27: 326–341.

Karsten U., Franklin L.A., Lüning K. & Wiencke C. 1998a. Natural ultraviolet radiation and photosynthetically active radiation induce formation of mycosporine-like amino acids in the marine macroalga *Chondrus crispus* (Rhodophyta). *Planta* 205: 257–262.

Karsten U., Sawall T., Hanelt D., Bischof K., Figueroa F.L., Flores-Moya A. & Wiencke C. 1998b. An inventory of UV-absorbing mycosporine-like amino acids in macroalgae from polar to warm-temperate regions. *Botanica Marina* 41: 443–453.

Klisch M. & Häder D.P. 2008. Mycsoporine-like amino acids and marine toxins – The common and the different. *Marine Drugs* 6: 147–163.

Korbee N., Mata M. & Figueroa F. 2010. Photoprotection mechanisms against ultraviolet radiation in *Heterocapsa* sp. (Dinophyceae) are influenced by nitrogen availability: Mycosporine-like amino acids vs. xanthophyll cycle. *Limnology and Oceanography* 55: 899–908.

Laviale M. & Neveux J. 2011. Relationships between pigment ratios and growth irradiance in 11 marine phytoplankton species. *Marine Ecology Progress Series* 425: 63–77.

Moeller R.E., Gilroy S., Williamson C.E., Grad G. & Sommaruga R. 2005. Dietary acquisition of photoprotective compounds (mycosporine-like amino acids, carotenoids) and acclimation to ulraviolet radiation in a freshwater copepod. *Limnology and Oceanography* 50: 427–439.

Moisan T.A. & Mitchell B.G. 2001. UV absorption by mycosporine-like amino acids in *Phaeocystis antarctica* Karsten induced by photosynthetically available radiation. *Marine Biology* 138: 217–227.

Moisan T.A., Olaizola M. & Mitchell B. 1998. Xanthophyll cycling in *Phaeocystis antarctica*: changes in cellular fluorescence. *Marine Ecology Progress Series* 169: 113–121.

Mushir S. & Fatma T. 2011. Ultraviolet radiation-absorbing mycsoporine like amino acids in cyanobacterium *Aulosira fertilissima*: Environmental perspective and characterization. *Current Research Journal of Biological Science* 3: 165–171.

Neals P.J., Banaszak A.T. & Jarriel C.R. 1998. Ultraviolet sunscreens in *Gymnodinium sanguineum* (Dinophyceae): mycosporine-like amino acids protect against inhibition of photosynthesis. *Journal of Phycology* 34: 928–938.

Park M.O. 2006. Composition and distribution of phytoplankton with size fraction results at southwestern East/Japan Sea. *Ocean Science Journal* 41: 301–313.

Pfündel E.E., Pan R.S. & Dilley P.A. 1992. Inhibition of violaxanthin deepoxidation by ultraviolet-B radiation in isolated chloroplasts and intact leaves. *Plant Physiology* 98: 1372–1380.

Portwich A. & Garcia-Pichel F. 1999. Ultraviolet and osmotic stresses induce and regulate the synthesis of mycosporines in the cyanobactrium *Chlorogloeopsis* PCC 6912. *Archives of Mcrobiology* 172: 187–192.

Rech M., Mouget J.L., Morant-Manceau A., Rosa P. & Tremblin G. 2005. Long-term acclimation to UV radiation: effects on growth, photosynthesis and carbonic anhydrase activity in marine diatoms. *Botanica Marina* 48: 407–420.

Riegger L. & Robinson D. 1997. Photoinduction of UV-absorbing compounds in Antarctic diatoms and *Phaeocystis Antarctica*. *Marine Ecology Progress Series* 160: 13–25.

Shick J.M., Lesser M.P. & Stochaj W.R. 1991. Ultraviolet radiation and photooxidative stress in zooxanthellate Anthozoa: the sea anemone *Phyllodiscus semoni* and the octocoral *Clavularia* sp.. *Symbiosis* 10: 145–173.

Shick J.M., Romaine-Lioud S., Ferrier-Pages C. & Gattuso J.P. 1999. Ultraviolet-B radiation stimulates shikimate pathway dependent accumulation of mycosporine-like amino acids in the coral *Stylophora pistillata* despite decreases in its population of symbiotic dinoflagellates. *Limnology and Oceanography* 44: 1667–1682.

Sinha R.P. & Häder D.P. 2002. Life under solar UV radiation in aquatic organisms. *Advances in Space Research* 30: 1547–1556.

Sinha R.P., Ambasht N.K., Sinha J.P., Klisch M. & Häder D.P. 2003. UV-B-induced synthesis of mycosporine-like amino acids in three strains of *Nodularia* (cyanobacteria). *Journal of Photochemistry and Photobiology B: Biology* 71: 51–58.

Sinha R.P., Klish M., Helbling E.W. & Häder D.P. 2001. Induction of mycosporine-like amino acids (MAAs) in cyanobacteria by solar ultraviolet-B radiation. *Journal of Photochemistry and Photobiology B: Biology* 60: 12–135.

Sinha R.P., Singh S.P. & Häder D.P. 2007. Database on mycosporines and mycosporine-like amino acids (MAAS) in fungi, cyanobacteria, macroalgae, phytoplankton and animals. *Journal of Photochemistry and Photobiology B: Biology* 89: 29–35.

Takahashi K., Wada E. & Sakamoto M. 1991. Relationship between carbon isotope discrimination and the specific growth rate of green alga, *Chlamydomonas reinhardtii*. *Japanese Journal of Limnology* 52: 105–112.

Taylor F., Mcminn A. & Franklin D. 1997. Distribution of diatoms in surface sediments of Prydz Bay, Antarctica. *Marine Micropaleontology* 32: 209–229.

Vernet M., Brody E.A., Holm-Hansen O. & Mitchell B.G. 1994. The response of Antarctic phytoplankton to ultraviolet light: absorption, photosynthesis, and taxonomic composition. *Antarctic Research Series* 62: 143–158.

Volkmann M. & Gorbushina A.A. 2006. A broadly applicable method for extraction and characterization of mycosporines and mycosporine-like amino acids of terrestrial, marine and freshwater origin. *FEMS Microbiology Letters* 255: 286–295.

Wängberg S.´Å., Andreasson K., Garde K., Gustavson K., Henriksen P. & Reinthaler T. 2006. Inhibition of primary production by UV-B radiation in an arctic bay - model calculations. *Aquatic Sciences* 68: 117–128.

Whitehead K., Karentz D. & Hedges J. 2001. Mycosporine-like amino acids (MAAs) in phytoplankton, a herbivorous pteropod (*Limacina helicina*), and its pteropod predator (*Clione antarctica*) in McMurdo Bay, Antarctica. *Marine biology* 139: 1013–1019.

Zielinski U. & Gersonde R. 1997. Diatom distribution in Southern Ocean surface sediments (Atlantic sector): implications for palaeoenvironmnetal reconstructions. *Palaeogeography, Palaeoclimatology, Palaeoecology* 129: 213–250.

Zudaire L. & Roy S. 2001. Photoprotection and long-term acclimation to UV radiation in the marine diatom *Thalassiosira weissflogii*. *Journal of Photochemistry and Photobiology B: Biology* 62: 26–34.